Journal of Engineering Mathematics, Vol. 14, no. 4, October 1980

Printed in the Netherlands

Flapping response of lifting rotor blades to spanwise nonuniform random excitation*

F. Y. M. WAN

Department of Mathematics and Institute of Applied Mathematics and Statistics, The University of British Columbia, Vancouver, B.C., V6T 1W5 Canada

(Received July 1, 1979 and in revised form November 1, 1979)

SUMMARY

Second-order rigid flapping response statistics of lifting rotor blades are obtained by a *spatial correlation method* for a general linear PDE with random forcing previously formulated by the author. These statistics enable us to analyze the effect of a finite correlation length of a spanwise nonuniform random excitation on the flapping blade response. For a random vertical inflow typical of turbulence excitation and for an advance ratio small compared to unity, this effect can be concisely expressed in terms of an *amplitude factor* and a *phase factor*. In the case of a spanwise correlation length of the order of the blade length, the amplitude factor shows that there may be as much as a 40% error in a solution which assumes the inflow is spatially uniform. The analytical development for a multi-mode solution illustrates how the *spatial correlation method* may be used in conjunction with a Galerkin procedure.

1. Introduction

The dynamics of flexible lifting rotor blades in forward flight (Fig. 1) is complicated by the fact that the aerodynamic lift acting on the blade changes significantly in the course of each blade revolution. Even an analysis of the small-amplitude motion of such a structure must cope with problems such as parametric excitation associated with the periodically time-varying system parameters which characterize the aerodynamic damping and spring-force effects. In one model for the forced small transverse vibration of a single blade, the dimensionless transverse displacement $w(x,\tau)$ (normalized by the blade length l) is governed by the dimensionless partial differential equation [1, 2, 9]

$$w_{\tau\tau} + \gamma_0 |x + \mu\sin\tau| w_\tau + L_{x\tau}[w] = f(x,\tau) \qquad (0 < x < 1, \tau > 0) \tag{1}$$

with

$$L_{x\tau}[\ ] = \zeta^4 [\ ]_{xxxx} - \tfrac{1}{2}(1 - x^2)[\ ]_{xx} + (x + \gamma_0\mu\cos\tau |x + \mu\sin\tau|)[\ ]_x \tag{2}$$

where $\gamma \equiv 6\gamma_0$ is the *Lock number* characterizing the aerodynamic effect, μ is the *advance ratio* (the ratio of the forward speed of the vehicle, V_f, to the rotating speed at the blade tip, Ωl),

* The research was supported in part by the Army Materials and Mechanics Research Center of Watertown, Mass., U.S.A. (Contract No. DAAG46-73-C-0227) and in part by the National Science and Engineering Research Council of Canada under Operating Grant No. A9259.

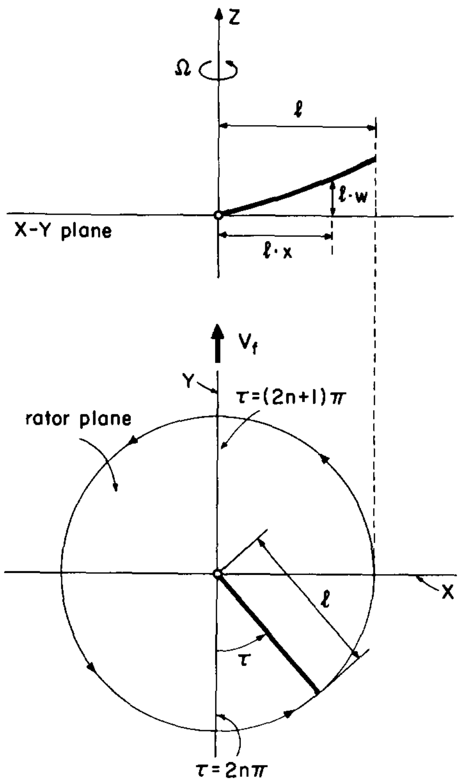

Figure 1. Schematic diagram of a rotor blade.

x is the distance from the axis of rotation along the blade span normalized by the blade length, and τ/Ω is the real time. The effective bending stiffness factor of the blade, ζ^4, is related to the bending stiffness of the uniform blade, EI, by the relation $\zeta^4 = EI/ml^4\Omega^2$, where m is the blade mass per unit blade length. When the source of external excitation is a vertical inflow, we have $f(x,\tau) = \gamma_0 | x + \mu \sin\tau | \lambda(x,\tau)$ where λ is the so-called *inflow ratio*. The temporally periodic coefficients in the PDE (1) give rise to the possibility of parametric excitation and dynamic instability (see [1] and references therein).

Aside from the various stability analyses, there is also the problem of the effect of random air and rotor generated turbulence on the structural integrity of the blade. In an effort to understand this aspect of the rotor blade problem, several papers in the literature analyze the stochastic blade response to a (zero mean) random inflow with known statistics (see [2] and references given therein). Because of the time-varying coefficients in (1), the steady-state response process $w(x,\tau)$ will be temporally nonstationary even if $\lambda(x,\tau)$ is stationary. In spite of the substantial reduction (by at least an order of magnitude) in machine computation made possible by a new method of solution developed in [3] and used in [2], it is still rather expensive to generate useful information on the stochastic properties of the nonstationary steady-state response of the flexible blade for design purpose.

For a blade hinged at the axis of rotation and free at the other end, we have

$$w(0,\tau) = w_{xx}(0,\tau) = w_{xx}(1,\tau) = w_{xxx}(1,\tau) = 0. \tag{3}$$

If the inflow is uniform along the blade span so that $\lambda(x,\tau)$ is independent of x, one may expect that the dominant motion of such a blade is in the form of rigid flapping. A solution of the stochastic forced transverse vibration problem for a *spanwise uniform* loading based on a rigid flapping blade model is considerably simpler than a more general flexible blade analysis as far as the amount of required machine computation is concerned (see [4] and [5]). Inasmuch as the stochastic loadings experienced by rotor blades are often random functions of both space and time, a rigid flapping solution for (zero mean) spanwise correlated random loads of comparable simplicity should be of interest (as pointed out in [4]). The rigid flapping mode of blade deformation is the lowest among the normal modes of a steadily rotating beam, i.e., for the linear operator (2) with $\mu = 0$ and the boundary conditions (3). Such a solution and the string solution ($\zeta^4 = 0$) of [2] delimit the range of the solution for any flexible blade with finite bending stiffness. With the help of the spatial correlation method of [3], we can now formulate an efficient computational procedure to obtain the rigid flapping mode solution for a spanwise correlated random excitation containing as a special case the solution of [4] and [5] for spanwise uniform inflows. The results obtained show that ignoring a finite spanwise load correlation length may have an unexpectedly significant effect on the second-order response statistics of the blade, even for the rigid flapping mode. At the same time, the analytical development leading to these results illustrates how the general *spatial correlation method* may be used in conjunction with a Galerkin procedure.

For the purpose of illustrating our method of solution, we take $\lambda(x,\tau)$ to be of zero mean and exponentially correlated in time with an autocorrelation function

$$<\lambda(x_2,\tau_2)\,\lambda(x_1,\tau_1)> = e^{-\alpha|\tau_2-\tau_1|}R_S(x_2,x_1) \tag{4}$$

where $<\ldots>$ is the *ensemble-averaging* operation, α is a known positive constant and $R_S(x_2,x_1) = R_S(x_1,x_2)$ is a given function. $R_S(x_1,x_2)$ was taken to be a positive constant σ^2 for the case of a random inflow due to high-altitude air turbulence in [4]. Since equation (1) is linear (so are the associated initial and boundary conditions), $w(x,\tau)$ is also of zero mean and we can therefore concentrate on the second-order response statistics of $w(x,\tau)$ characterized by the autocorrelation function $R(x_2,\ \tau_2;\ x_1,\ \tau_1) = <w(x_2,\ \tau_2)\ w(x_1,\ \tau_1)>$. To determine $R(x_2,\tau_2;x_1,\tau_1)$, we will follow the procedure of [2, 3] and consider $\lambda(x,\tau)$ to be the steady-state stationary response to a temporally uncorrelated random excitation $n(x,\tau)$ of a dynamical system characterized by the first order ODE

$$\lambda_\tau + \alpha\lambda = \sqrt{2\alpha}\,n(x,\tau) \tag{5}$$

where $<n(x_2,\ \tau_2)\ n(x_1,\ \tau_1)> = R_S(x_2,\ x_1)\ \delta(\tau_2-\tau_1)$. It is not difficult to verify that the autocorrelation function of the steady-state solution of (5) is as given by the right-hand side of (4) (see [2]). Furthermore, it can be shown [2] that

$$<n(y,\tau')\,w(x,\tau)> = <n(y,\tau')\,w_\tau(x,\tau)> = 0 \tag{6}$$

for all $\tau' \geqslant \tau > 0$ and $0 \leqslant x,\ y \leqslant 1$. The numerical results to be given in this paper will be for the special case $R_S(x,y) = \sigma^2\exp(-\epsilon|x\text{-}y|)$ where $\sigma^2 > 0$ and $\epsilon \geqslant 0$ are given constants.

The analytical and numerical results for the rigid flapping solution obtained with the help of the above device allow us to study the effect of a finite load-correlation length characterized by the dimensionless number ϵ (with the correlation length equal to l/ϵ) on the second-order statistics of the (zero mean) rigid flapping blade response. In the low advance ratio range, $\mu^3 << 1$, a perturbation solution shows that the effect of the correlation length may be completely described by an *amplitude factor* ρ and a *phase factor* ψ, both factors are simple functions of ϵ. In the case of a random vertical inflow with a correlation length of the order of the blade length ($\epsilon = O(1)$), we see from the expression for $\rho(\epsilon)$ that the discrepancy between our solution and one ignoring the finite spatial load-correlation (as in [4] and [5]) may be as much as 40% of the former. In the high advance ratio range, an efficient numerical solution procedure is formulated for the second-order statistics of the periodic steady-state flapping blade response. The numerical solution obtained by this efficient procedure shows that the effect of a finite load-correlation length ($0 < \epsilon < \infty$) is qualitatively similar to that described by the amplitude and phase factor for the low advance ratio case.

2. Spatial correlation functions for flexible blade response

The essential feature of the spatial correlation method for the second-order response statistics proposed in [3] and used in [2] and [6] is the formulation of a nonstochastic mixed initial-boundary value problem for the four unknown *spatial correlation functions* of the response proces $w(x,\tau)$:

$$\begin{aligned} u(x,y,\tau) &= \langle w(x,\tau)\, w(y,\tau) \rangle, \qquad & s(x,y,\tau) &= \langle w(x,\tau)\, w_\tau(y,\tau) \rangle, \\ t(x,y,\tau) &= \langle w_\tau(x,\tau)\, w(y,\tau) \rangle, \qquad & v(x,y,\tau) &= \langle w_\tau(x,\tau)\, w_\tau(y,\tau) \rangle, \end{aligned} \tag{7}$$

for all $0 \leqslant x,\ y \leqslant 1$ and $\tau \geqslant 0$. Note that these spatial correlation functions contain the mean-square response properties as special cases (when $y = x$). As we shall see, they also serve as the initial conditions for a nonstochastic mixed initial boundary value problem for the determination of the autocorrelation function $R(x_2, \tau_2; x_1, \tau_1)$, (Section 7).

To obtain an appropriate set of equations for u, s, t and v, we observe that

$$u_\tau = \langle w_\tau(x,\tau)\, w(y,\tau) \rangle + \langle w(x,\tau)\, w_\tau(y,\tau) \rangle = t + s \tag{8}$$

and

$$t_\tau = v(x,y,\tau) + \langle w_{\tau\tau}(x,\tau)\, w(y,\tau) \rangle \tag{9}$$

where we have made use of the fact that, within the framework of meansquare convergence, differentiation commutes with the ensemble-averaging operation. We now use equation (1) to eliminate $w_{\tau\tau}$ from (9) so that

$$t_\tau = v - L_{x\tau}[u] - \gamma_0\, |x + \mu\sin\tau|\, t + \hat{p}(x,y,\tau) \tag{10}$$

where

$$\begin{aligned} \hat{p}(x,y,\tau) &= \gamma_0\, |x + \mu\sin\tau| \langle \lambda(x,\tau)\, w(y,\tau) \rangle \\ &\equiv \gamma_0\, |x + \mu\sin\tau|\, p(x,y,\tau). \end{aligned} \tag{11}$$

Interchange the role of x and y and we have also

$$s_\tau = v - L_{y\tau}[u] - \gamma_0 |y + \mu\sin\tau| s + \hat{p}(y,x,\tau). \tag{12}$$

Finally, similar manipulations applied to the expression for v_τ give

$$v_\tau = - L_{x\tau}[s] - L_{y\tau}[t] - \gamma_0(|x + \mu\sin\tau| + |y + \mu\sin\tau|)\, v + \hat{q}(x,y,\tau) \tag{13}$$

where

$$\hat{q}(x,y,\tau) = \gamma_0 |x + \mu\sin\tau| q(x,y,\tau) + \gamma_0 |y + \mu\sin\tau| q(y,x,\tau) \tag{14}$$

with $q(x,y,\tau) = < \lambda(x,\tau)\, w_\tau(y,\tau) >$.

Equations (8), (10), (12) and (13) are to be satisfied in the interior of the semi-infinite unit square column $(0 < x,\ y < 1,\ \tau > 0)$ in the $x,\ y,\ \tau$-space. On the base square of the column, $\tau = 0$, we have from the condition of no initial transverse motion:

$$W(x,y,0) = 0, \qquad W \equiv \begin{bmatrix} u & s \\ t & v \end{bmatrix} \qquad (0 \leqslant x,\ y \leqslant 1). \tag{15}$$

The appropriate boundary conditions on the four walls of the column are obtained from (3) and (7):

$$\begin{aligned} &W(0,y,\tau) = W_{xx}(0,y,\tau) = W_{xx}(1,y,\tau) = W_{xxx}(1,y,\tau) = 0, \quad (0 \leqslant y \leqslant 1,\ \tau > 0), \\ &W(x,0,\tau) = W_{yy}(x,0,\tau) = W_{yy}(x,1,\tau) = W_{yyy}(x,1,\tau) = 0, \quad (0 \leqslant x \leqslant 1,\ \tau > 0). \end{aligned} \tag{16}$$

The four equations (8), (10), (12) and (13) contain six unknowns since $p(x,y,\tau)$ and $q(x,y,\tau)$ involve the unknown w. We need two more equations to complete the system. To get these, we observe that

$$\begin{aligned} p_\tau(x,y,\tau) &= < \lambda_\tau(x,\tau)\, w(y,\tau) > + < \lambda(x,\tau)\, w_\tau(y,\tau) > \\ &= - \alpha p(x,y,\tau) + q(x,y,\tau) \end{aligned} \tag{17}$$

and

$$\begin{aligned} q_\tau(x,y,\tau) &= < \lambda_\tau(x,\tau)\, w_\tau(y,\tau) > + < \lambda(x,\tau)\, w_{\tau\tau}(y,\tau) > \\ &= - (\alpha + \gamma_0 |y + \mu\sin\tau|)\, q(x,y,\tau) - L_{y\tau}[p(x,y,\tau)] \\ &\quad + \gamma_0 |y + \mu\sin\tau| R_S(x,y) \end{aligned} \tag{18}$$

where we have made use of the PDE (1) to eliminate $w_{\tau\tau}$, the ODE (5) to eliminate λ_τ, and the conditions (6) to simplify the resulting equations. The initial conditions

$$p(x,y,0) = q(x,y,0) = 0, \quad (0 \leqslant x,\ y \leqslant 1) \tag{19}$$

supplementing (17) and (18) follow from the fact that the blade experiences no transverse (out of the rotor plane) motion up to some reference time $\tau = 0$. The boundary conditions for p and q follow from (3) and the definition of p and q:

$$p(x,0,\tau) = p_{yy}(x,0,\tau) = p_{yy}(x,1,\tau) = p_{yyy}(x,1,\tau) = 0, \quad (0 \leqslant x \leqslant 1, \tau > 0). \tag{20}$$

We can first solve (17-20) for p and q in the y,τ-space with x as a parameter, and then use the result in (8), (10), (12) and (13) for the determination of the other four unknowns. We note also that the spatial correlation of the loading, characterized by $R_S(x,y)$, enters into the analysis explicitly only through its appearance on the right side of (18).

3. The rigid flapping motion

We now introduce the rigid flapping assumption by taking $w(x,\tau) = x\phi(\tau)$, so that

$$\begin{aligned} u(x,y,\tau) &= xyU(\tau), \qquad & s(x,y,\tau) &= xyS(\tau),\\ t(x,y,\tau) &= xyT(\tau), \qquad & v(x,y,\tau) &= xyV(\tau), \end{aligned} \tag{21}$$

where $U(\tau) = \langle \phi^2(\tau) \rangle$, etc., and equations (8), (10), (12) and (13) become four ODE:

$$\begin{aligned} \dot{U} &= T + S,\\ \dot{T} &= V - [\omega^2 + k(\tau)]\,U - c(\tau)\,T + P(\tau),\\ \dot{S} &= V - [\omega^2 + k(\tau)]\,U - c(\tau)\,S + P(\tau),\\ \dot{V} &= -[\omega^2 + k(\tau)]\,(S + T) - 2c(\tau)\,V + 2Q(\tau), \end{aligned} \tag{22}$$

where $\dot{(\;)} \equiv d(\;)/d\tau$ and where

$$\begin{aligned} k(\tau) &= 3\gamma_0 \mu \cos\tau \int_0^1 |x + \mu\sin\tau|\, x\,dx,\\ c(\tau) &= 3\gamma_0 \int_0^1 |x + \mu\sin\tau|\, x^2\,dx \end{aligned} \tag{23}$$

and

$$\{P(\tau), Q(\tau)\} = 3\gamma_0 \int_0^1 x\,|x + \mu\sin\tau|\, \{\bar{p}(x,\tau), \bar{q}(x,\tau)\}\,dx \tag{24}$$

with

$$\begin{aligned} \{\bar{p}(x,\tau), \bar{q}(x,\tau)\} &= 3\int_0^1 y\{p(x,y,\tau), q(x,y,\tau)\}\,dy\\ &= \{\langle \lambda(x,\tau)\,\phi(\tau)\rangle, \langle \lambda(x,\tau)\,\dot{\phi}(\tau)\rangle\}. \end{aligned} \tag{25}$$

The constant ω^2 is equal to 1 since the blade is hinged at the blade root (but would be greater than unity for a blade with an elastic root restraint). Note that the expressions in (21) satisfy the boundary conditions (16).

The quantities $\bar{p}\ (x,\tau)$ and $\bar{q}\ (x,\tau)$ are determined by

$$\bar{p}_\tau = -\alpha\bar{p} + \bar{q},\ \bar{q}_\tau = -[\alpha + c(\tau)]\bar{q} - [\omega^2 + k(\tau)]\bar{p} + \bar{r}(x,\tau), \tag{26}$$

$$\bar{p}(x,0) = \bar{q}(x,0) = 0 \tag{27}$$

where

$$\bar{r}(x,\tau) = 3\gamma_0 \int_0^1 y\,|y + \mu\sin\tau|\,R_S(x,y)\,dy. \tag{28}$$

Equations (26) are obtained from (17) and (18) by multiplying through by $3y$ and integrating over the interval (0,1). Note that with $w(y,\tau) = y\phi(\tau)$, $p(x,y,\tau)$ satisfies the boundary conditions (20).

The general procedure is to solve the initial-value problem (26) and (27) with x as a parameter. The results are to be used in the integrals on the right side of equations (24) and the integrals evaluated to give $P(\tau)$ and $Q(\tau)$. Having P and Q, we can then solve the four equations (22) subject to the initial conditions

$$U(0) = S(0) = T(0) = V(0) = 0 \tag{29}$$

which follow from (15). We note, however, that the second and third equation of (22) together with $S(0) = T(0) = 0$ imply $S(\tau) = T(\tau)$ for all τ (consistent with the fact $S = \langle \phi\dot{\phi} \rangle = T$). Therefore, the system (22) is effectively a system of three equations

$$\begin{aligned} \dot{U} &= 2S,\quad \dot{S} = V - [\omega^2 + k(\tau)]\,U - c(\tau)\,S + P, \\ \dot{V} &= -2[\omega^2 + k(\tau)]\,S - 2c(\tau)\,V + 2Q. \end{aligned} \tag{30}$$

The damping coefficients $c(\tau)$ and the supplementary spring rate $k(\tau)$ due to the aerodynamic lift have been calculated in [9]. In the case where λ is independent of x, we have $R_S(x,y) = \sigma^2$ (a positive constant); the corresponding $\bar{r}(x,\tau) = \bar{r}(\tau)$ reduces to the envelope function for the inflow ratio term given in [9].

4. Exponential correlation in space-hovering

In the remaining sections of this paper, we restrict ourselves to the class of random excitations with

$$R_S(x,y) = \sigma^2 e^{-\epsilon|x-y|} \tag{31}$$

where $\sigma^2 > 0$ and $\epsilon \geqslant 0$ are known constants with $1/\epsilon$ being the load correlation length. We will be interested in how the rigid-blade solutions obtained in [4], [5] and [7] for a spatially uniform random excitation are modified by a finite load-correlation length. In this section, we consider first the simpler case of hovering.

With $\mu = 0$, equations (26) become

$$\bar{p}_\tau = -\alpha\bar{p} + \bar{q}, \quad \bar{q}_\tau = -(\alpha + \frac{\gamma}{8})\bar{q} - \omega^2\bar{p} + \bar{r} \tag{32}$$

where

$$\begin{aligned}\bar{r} &= 3\gamma_0\sigma^2\int_0^1 y^2 e^{-\epsilon|x-y|}dy \\ &= \frac{\gamma\sigma^2}{\epsilon^3}\,[2x^2 + \epsilon^2x^4 - x^2e^{-\epsilon x} - x^2e^{\epsilon(x-1)}(1+\epsilon+\frac{\epsilon^2}{2})].\end{aligned} \tag{33}$$

Since $\bar{r}$ is independent of τ, the steady-state solution of (32), denoted by $\bar{p}_s$ and $\bar{q}_s$, is also independent of τ and can be obtained simply by setting $\bar{p}_\tau = \bar{q}_\tau = 0$. The resulting algebraic equations give

$$\bar{p}_s = \bar{r}(x)/\Delta, \quad \bar{q}_s = \alpha\bar{p}_s, \quad \Delta = \omega^2 + a^2 + \alpha\gamma/8. \tag{34}$$

Correspondingly, we have from (24)

$$\begin{aligned}P_s &= 3\gamma_0\int_0^1 x^2\bar{p}_s(x)dx = \frac{\gamma^2\sigma^2}{36\Delta}\,\rho(\epsilon),\ Q_s = \alpha P_s, \\ \rho(\epsilon) &= \frac{72}{\epsilon^6}\,[e^{-\epsilon}(1+\epsilon+\frac{\epsilon^2}{2}) - (1 - \frac{\epsilon^3}{6} + \frac{\epsilon^4}{8} - \frac{\epsilon^5}{20})]\end{aligned} \tag{35}$$

which are also independent of τ. It follows that the steady-state solution of (30), denoted by $\bar{U}$, $\bar{S}$ and $\bar{V}$, is also independent of τ. By setting $U_\tau = V_\tau = S_\tau = 0$, we have immediately from (30):

$$\begin{aligned}\bar{V} &= \frac{8\alpha}{\gamma}\,P_s = \frac{2\alpha\gamma\sigma^2}{9\Delta}\rho(\epsilon) \equiv V_0\rho(\epsilon), \\ \bar{U} &= \frac{\gamma\sigma^2(8a+\gamma)}{36\Delta\omega^2}\rho(\epsilon) \equiv U_0\rho(\epsilon), \quad \bar{S} = 0,\end{aligned} \tag{36}$$

where V_0 and U_0 are independent of ϵ and are in fact the meansquare velocity and displacement known for the case of a spanwise uniform random inflow with the same exponential time-correlation [4, 5, 7]. The factor $\rho(\epsilon)$ in (32) and (33) may therefore be thought of as an *amplitude factor* associated with a finite spanwise correlation length of the inflow. It is not difficult to verify that $\rho(\epsilon) \to 1$ and $\rho'(\epsilon) \to 0$ as $\epsilon \to 0$ so that $\bar{V}/V_0$ and $\bar{U}/U_0$ decrease with increasing

ϵ for small ϵ. A small but positive ϵ means a finite correlation length which is large compared with the blade length. On the other hand, $\rho(\epsilon) \to 0$ and $\frac{1}{2}\epsilon\rho(\epsilon) \to 9/5$ as $\epsilon \to \infty$, so that the solution tends to that of a spatially delta-correlated inflow. The variation of the amplitude factor $\rho(\epsilon)$ over the whole range of ϵ is given in Figure 2 where we have plotted $\epsilon\rho(\epsilon)/2$ for all $\epsilon > 2$ in order to compare with the limiting case of spanwise delta-correlated inflow. The plot shows that ρ is a monotone decreasing function as ϵ increases. Therefore, the meansquare flapping displacement and velocity decrease with *decreasing* spanwise correlation length of the particular class of inflows.

For blades in hover, the problem with a random inflow excitation is a rather artificial one; instead, an excitation due to a randomly changing collective pitch angle $\theta(x,\tau)$ is of interest. For this case, we have $f(x,\tau) = \gamma_0 |x + \mu \sin\tau|^2\ \theta(x,\tau)$. If $\theta(x,\tau)$ is exponentially correlated both in space and time (as given by (4) and (31)), similar calculations for $\mu = 0$ give

$$\bar{V} = \frac{2\alpha\gamma\sigma^2}{16\Delta}\rho_\theta(\epsilon),\quad \bar{U}_\theta = \frac{\gamma\sigma^2(8\alpha+\gamma)}{64\Delta\omega^2}\rho_\theta(\epsilon),\quad \bar{S}_\theta = 0, \tag{37}$$

$$\rho_\theta(\epsilon) = \frac{1152}{\epsilon^8}[(1 - \frac{\epsilon^4}{24} + \frac{\epsilon^5}{30} - \frac{\epsilon^6}{72} + \frac{\epsilon^7}{252} - e^{-\epsilon}(1 + \epsilon + \frac{\epsilon^2}{2!} + \frac{\epsilon^3}{3!})] \tag{38}$$

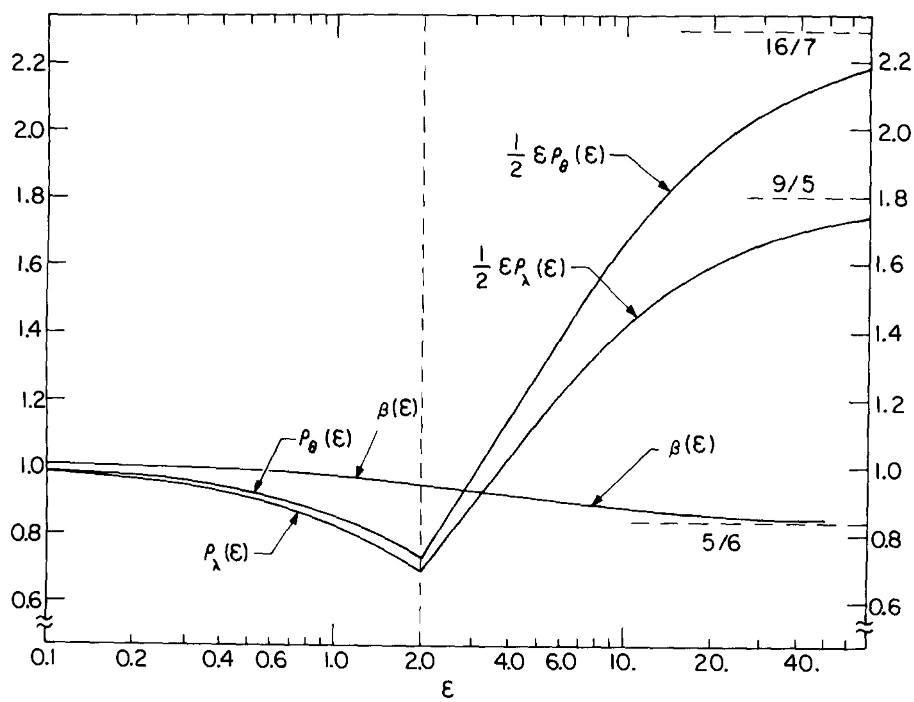

Figure 2. Amplitude and phase factor.

and where Δ is as given in (33). The variation of ρ_θ with ϵ is also shown in Figure 2. With $\rho_\theta(\epsilon) \to 1$ as $\epsilon \to 0$, the results in (37) tend to those for a spanwise uniform θ obtained in [7]. As $\epsilon \to \infty$, $\rho_\theta(\epsilon)$ tends to zero while $\frac{1}{2}\epsilon\rho_\theta(\epsilon)$ tends to 16/7 corresponding to the case $R_S(x,y) = \sigma^2\delta(x-y)$. For finite values of ϵ, $\rho_\theta(\epsilon)$ is again a monotone decreasing function as ϵ increases. Therefore, the meansquare flapping displacement and velocity are also reduced by a shortening of the spanwise correlation length of this particular class of $\theta(x,\tau)$.

Before leaving the hovering case, it should be noted that the quantities V_0 and U_0 (for both kinds of random excitations considered) are monotone increasing functions of γ for all $\gamma \geqslant 0$ and for all positive values of ω^2 and α. In the realistic range of γ and ω^2, V_0 increases almost linearly with γ while U_0 increases quadratically with γ for $\alpha = O(1)$ and is only (nearly) linear in γ for broad band excitations ($\alpha >> 1$).

5. Forward flight at low advance ratios

While an exact elementary solution of our problem was obtained in Section 4 for the hover case ($\mu = 0$), the same is not possible for the forward-flight case ($\mu > 0$). To gain some insight into the effect of a spanwise correlation of the inflow, we restrict ourselves in this section to the *low* advance-ratio range, i.e., $\mu^3 \ll 1$. As expected, the contribution of the reverse-flow effect can be neglected (see [4, 8]) in this range so that

$$\begin{aligned}
c(\tau) &\cong 3\gamma_0 \int_0^1 (x^3 + x^2 \mu\sin\tau)dx = \frac{\gamma}{8} + \frac{\gamma}{6}\mu\sin\tau \equiv c_n(\tau),\\
k(\tau) &\cong 3\gamma_0\mu\cos\tau \int_0^1 (x^2 + x\mu\sin\tau)dx\\
&= \frac{\gamma}{6}\mu\cos\tau + \frac{\gamma}{8}\mu^2\sin 2\tau \equiv k_n(\tau),\\
\bar{r}(x,\tau) &\cong 3\gamma_0\sigma^2 \int_0^1 (y^2 + y\mu\sin\tau)\, e^{-\epsilon|x-y|}dy\\
&= \sigma^2\gamma[r_0(x) + r_1(x)\,\mu\sin\tau] \equiv r_n(x,\tau),
\end{aligned} \tag{39}$$

where the subscript n indicates a normal flow situation and where

$$\begin{aligned}
r_0(x) &= \epsilon^{-3}[2 + \epsilon^2x^2 - e^{-\epsilon x} - e^{-\epsilon(1-x)}(1 + \epsilon + \tfrac{1}{2}\epsilon^2)],\\
r_1(x) &= \tfrac{1}{2}\epsilon^{-2}[2\epsilon x + e^{-\epsilon x} - e^{-\epsilon(1-x)}(1 + \epsilon)].
\end{aligned} \tag{40}$$

The form of $c_n(\tau)$, $k_n(\tau)$ and $r_n(x,\tau)$ suggests that a *steady-state* solution of (17) and (18) in powers of μ is possible when $\mu < 1$.* Upon writing

* A perturbation solution of the initial-value problem (15)-(17) itself can be obtained without difficulty. But we are not interested here in the transient part of the meansquare response properties. By retaining terms of higher powers of μ in (39), (41) and (45), the same solution technique also gives results for moderate advance ratios, i.e. $\mu < 1$.

$$\{\bar{p},\bar{q}\} = \sum_{m=0}^{\infty} \{p_m(x,\tau),q_m(x,\tau)\}\mu^m, \tag{41}$$

the coefficients p_m and q_m (which are independent of μ) are evidently the particular solutions of the following sequence of ODE:

$$\ddot{p}_0 + 2c_0\dot{p}_0 + \Delta p_0 = \gamma r_0(x), \quad q_0 = \dot{p}_0 + \alpha p_0; \tag{42a}$$

$$\begin{cases} \ddot{p}_1 + 2c_0\dot{p}_1 + \Delta p_1 = \gamma r_1(x)\sin\tau - \dfrac{\gamma}{6}\sin\tau \dot{p}_0 - \dfrac{\gamma}{6}(\alpha\sin\tau + \cos\tau)p_0, \\ q_1 = \dot{p}_1 + \alpha p_1; \end{cases} \tag{42b}$$

etc.

where dots indicate differentiation with respect to τ, Δ is as defined in (34) and $c_0 = \alpha + \gamma/16$. It is a straightforward matter to obtain these particular solutions since the ODE involved are with constant coefficients.

The steady-state perturbation solutions (41) are then inserted into (24) with the reverse-flow effect neglected. Upon carrying out the integration, we get

$$\begin{aligned} P(\tau) &= \frac{\sigma^2\gamma^2}{36\Delta}\rho(\epsilon)\{1 + \mu[P_{s0} + P_{s1}\beta(\epsilon)]\sin\tau \\ &\qquad + \mu[P_{c0} + P_{c1}\beta(\epsilon)]\cos\tau + O(\mu^2)\}, \\ Q(\tau) &= \frac{\sigma^2\gamma^2}{36\Delta}\rho(\epsilon)\{\alpha + \mu[Q_{s0} + Q_{s1}\beta(\epsilon)]\sin\tau \\ &\qquad + \mu[P_{c0} + P_{c1}\beta(\epsilon)]\cos\tau + O(\mu^2)\} \end{aligned} \tag{43}$$

where $\rho(\epsilon)$ is as given in (32) and

$$\rho(\epsilon)\beta(\epsilon) = \frac{6}{\epsilon^3}\left[\left(1 - \epsilon + \frac{\epsilon^2}{2}\right) - e^{-\epsilon}\right] \tag{44}$$

The constants P_{sj}, P_{cj}, Q_{sj} and Q_{cj} depend only on γ, α and ω^2 and will not be listed here. Therefore, the effect of the spanwise correlation is completely described by the quantities $\rho(\epsilon)$ and $\beta(\epsilon)$. Note that we have $\beta(\epsilon) \to 1$ as $\epsilon \to 0$.

Having the steady-state solution for $P(\tau)$ and $Q(\tau)$, we can now use (30) to determine the steady-state meansquare properties of the blade response. In view of (43), a steady-state solution of (30) may be taken in the form

$$\{U,S,V\} = \{\bar{U},\bar{S},\bar{V}\} + \mu[\{U_s,S_s,V_s\}\sin\tau + \{U_c,S_c,V_c\}\cos\tau] + O(\mu^2). \tag{45}$$

The $O(1)$ terms, $\bar{U}$, $\bar{S}$ and $\bar{V}$, are just the steady-state solutions for the hover case given by (35). By the method of undetermined coefficients, the constants U_s, S_s, ..., V_c are solutions of a system of six coupled linear algebraic equations which may be written as two sets of three complex equations

$$\left(1+\frac{\gamma}{4}i\right)\widetilde{V}+\omega^2\widetilde{U}=2i\widetilde{Q}-\frac{\gamma}{3}i\widetilde{V},$$
$$-\widetilde{V}+\left(\omega^2-\frac{1}{2}-\frac{\gamma}{16}i\right)\widetilde{U}=\widetilde{P}+\frac{\gamma}{6}i\widetilde{U}, \tag{46}$$

$$\widetilde{U}-2i\widetilde{S}=0, \tag{47}$$

for the three complex unknown constants $\widetilde{U}$, $\widetilde{V}$ and $\widetilde{S}$ with

$$\{\widetilde{U},\widetilde{S},\ldots,\widetilde{Q}\}=\{U_s,\ldots,Q_s\}-i\{U_c,\ldots,Q_c\}, \tag{48}$$

$$\{P_s,P_c,Q_s,Q_c\}=\frac{\sigma^2\gamma^2}{36\Delta}\,\rho(\epsilon)[\{P_{s0},\ldots,Q_{c0}\}+\{P_{s1},\ldots,Q_{c1}\}\beta(\epsilon)]. \tag{49}$$

It follows from (33) and (45) that the solution of (43) and (44) can be put in the form

$$U_s=\sigma^2\rho(\epsilon)[U_{s0}+U_{s1}\beta(\epsilon)],\quad \text{etc.,} \tag{50}$$

where U_{s0}, U_{s1}, ..., V_{c1} depend only on γ, α and ω^2.

In the case $\epsilon = 0$, the solutions for the functions $U(\tau)$, $S(\tau)$ and $V(\tau)$ as given by (45) are exactly the approximate steady-state variances and covariance of the flapping response obtained in [8] for low advance-ratio flight and will be considered known. Our concern here is with the effect of a finite spanwise correlation length ($\epsilon > 0$) on these response statistics. This effect is completely described by the two quantities $\rho(\epsilon)$ and $\beta(\epsilon)$. From the plot of $\beta(\epsilon)$ in Figure 2, we see that this monotone decreasing function changes by less than 10% of its value at $\epsilon = 0$ as the correlation length shortens (from infinity) to a fraction of the blade length. Therefore, the main effect of a spanwise load correlation is in the amplitude factor $\rho(\epsilon)$. As both ρ and β decrease with increasing ϵ, a correlation-length shortening in the low advance-ratio range gives rise to a reduction in the time average of the meansquare flapping properties as well as in the fluctuation about these average values.

Solutions for $O(\mu^2)$-terms in (41) and (45) have also been obtained. In the $\epsilon = 0$ case, these terms involve the second harmonics cos 2τ and sin 2τ. The effect of a finite spatial correlation length on these $O(\mu^2)$-terms is qualitatively similar to that on the $O(1)$ and $O(\mu)$-terms. As such the explicit solutions for the $O(\mu^2)$-terms will not be listed here.

6. Numerical solution for arbitrary advance ratio

If μ^3 is not small compared to unity, the situation is much more complicated since the effect of reverse flow is no longer negligible. For $\mu \leqslant 1$, we have upon carrying out the integration in (23),

$$c(\tau)=\begin{cases} c_n(\tau), & (2m\pi\leqslant\tau\leqslant(2m+1)\pi) \\ c_n(\tau)+\dfrac{\gamma\mu^4}{96}(3-4\cos 2\tau+\cos 4\tau), & ((2m+1)\pi\leqslant\tau\leqslant(2m+2)\pi) \end{cases} \tag{51}$$

and

$$k(\tau) = \begin{cases} k_n(\tau), & (2m\pi \leqslant \tau \leqslant (2m+1)\pi) \\ k_n(\tau) - \dfrac{\gamma\mu^4}{48}\,(2\sin 2\tau - \sin 4\tau), & ((2m+1)\pi \leqslant \tau \leqslant (2m+2)\pi) \end{cases} \tag{52}$$

where m is any integer and the subscript n indicates a normal flow. Evidently, the effect of reverse flow is negligible in c and k if $\mu^3 \ll 1$ (in fact, as long as $\mu^4 \ll 1$). From (28), we get

$$\bar{r}(x,\tau) = \begin{cases} r_n(x,\tau), & (2m\pi \leqslant \tau \leqslant (2m+1)\pi,\ 0 \leqslant x \leqslant 1) \\ -r_n(x,\tau) - r_l(x,\tau), & ((2m+1)\pi \leqslant \tau \leqslant (2m+2)\pi,\ x \leqslant -\mu\sin\tau) \\ r_n(x,\tau) + r_g(x,\tau), & ((2m+1)\pi \leqslant \tau \leqslant (2m+2)\pi,\ x > -\mu\sin\tau) \end{cases} \tag{53}$$

where

$$r_l(x,\tau) = \gamma\epsilon^{-3}\{e^{-\epsilon(1-x)}[(2+2\epsilon+\epsilon^2)+\epsilon(1+\epsilon)\mu\sin\tau]$$

$$-e^{\epsilon(x+\mu\sin\tau)}(2-\epsilon\mu\sin\tau)\}, \tag{54}$$

$$r_g(x,\tau) = \gamma\epsilon^{-3}\{e^{-\epsilon x}(2-\epsilon\mu\sin\tau) - e^{-\epsilon(x+\mu\sin\tau)}(2+\epsilon\mu\sin\tau)\}.$$

With (53) and (54), it is not difficult to show that the effect of reverse flow can be neglected in $\bar{r}(x,\tau)$ if $\mu^3 \ll 1$ at least for $\epsilon \ll 1$ and $\epsilon \gg 1$.

For $\mu > 1$, the entire blade is subject to reverse flow in the range $-\sin\tau > \mu^{-1}$ so that

$$c(\tau) = -c_n(\tau), \quad k(\tau) = -k_n(\tau), \quad \bar{r}(x,\tau) = -r_n(x,\tau) \tag{55}$$

for all τ in the range $\frac{3\pi}{2} - \nu \leqslant \tau \leqslant \frac{3\pi}{2} + \nu$ where $\nu = \cos^{-1}(1/\mu)$. We can now solve the initial value problem, (26) and (27), numerically by a 4th-order Runge-Kutta scheme for a set of x values, say $x_0 = 0, x_1, x_2, \ldots, x_m = 1$. With $f_j(x_k) = f(x_k,\tau_j)$, the set of solutions $\{\bar{p}_j(x_k), \bar{q}_j(x_k)\}$ for a fixed j is used in (24) to get $P(\tau_j)$ and $Q(\tau_j)$ with the integrals evaluated by Simpson's rule. Once $P(\tau_j)$ and $Q(\tau_j)$ are calculated, the initial-value problem (29) and (30) is solved numerically again by a 4th-order Runge-Kutta schema. Within the stability boundaries of the two sets of equations, (26) and (30), we get accurate steady-state periodic solutions of the meansquare blade flapping properties after four blade revolutions for the realistic range of values of $\gamma(2 \leqslant \gamma \leqslant 12)$. For a fixed set of γ, μ, ϵ, α and ω^2, the entire solution process for P, Q, U, S and V consumes about 50 seconds on a UNIVAC 1106 if 21 stations along the blade span are used in the numerical evaluation of the integrals on the right side of (24).

With $R_S(x_2,x_1) = \sigma^2$ (a constant), the class of random functions characterized by (4) seems to adequately describe the random inflow associated with atmospheric turbulence at altitude higher than 300 ft. above terrain if the effect of the spatial variation of the vertical turbulence component, of the longitudinal turbulence component itself and of the blade motion are all neglected (see [4] and references therein). In that case, we have $\alpha = 2\mu l/L$ where l is the blade length and $L/2$ is the scale length of the vertical turbulence component. L is about 400 ft. for an altitude of 300-700 ft. above terrain and is several thousand feet for higher altitudes. From the expression for α, we see that, at the low advance-ratio range, the correlation time is long compared to one blade revolution for existing blades which range from 33 ft. to 100 ft. As such, the results of Section 5 for the low advance-ratio range serve only to indicate the qualitative effect of a spatially correlated inflow; we are mainly interested in the case of high advance-ratio flight.

The meansquare flapping responses of the blade to a zero mean $\lambda(x,\tau)$ with a correlation function given by (4) have been studied with the help of the numerical solution scheme outlined in this section for a wide range of the blade and load parameters. The numerical solution shows that the perturbation solution of Section 5 (including $O(\mu^2)$-terms) gives a very good approximation of the exact solution for $\mu \leqslant 0.4$. It also shows that the effect of a finite ϵ for all $0 \leqslant \mu \leqslant 1.6$ is qualitatively similar to that indicated by the perturbation solution. The actual distributions of the steade state $<\phi^2>$ and $<\dot{\phi}^2>$ are given in Figures 3, 4, 5 and 6 for $\mu = 1.6$ and for the two extreme rotor-disc sizes, $l = 33\frac{1}{3}$ ft. and $l = 100$ ft, operating at 300 ft. – 700 ft. above terrain (L = 400 ft.). We have taken $\omega^2 = 1$ in these examples since most existing blades are hinged at the blade root. We see that, aside from an increase in the magnitude of the meansquare response, an increase in μ tends to shift in the time when $<\phi^2>$ and $<\dot{\phi}^2>$ attain their maximum values further toward the midway point and the end of the backstroke, respectively.

Finally, we show in Tables 1 and 2 the effect of the Lock number γ on the peak values of $<\phi^2>$ and $<\dot{\phi}^2>$. We see in particular that the amplitude growth with γ is nonlinear and the growth rate depends significantly on μ but not at all on ϵ.

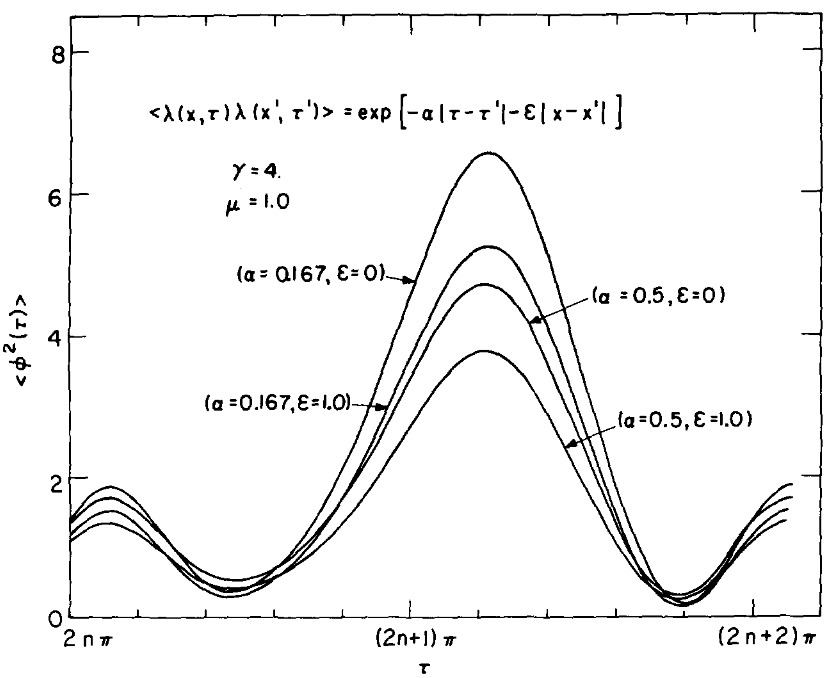

Figure 3. Meansquare flapping angle (μ = 1.0).

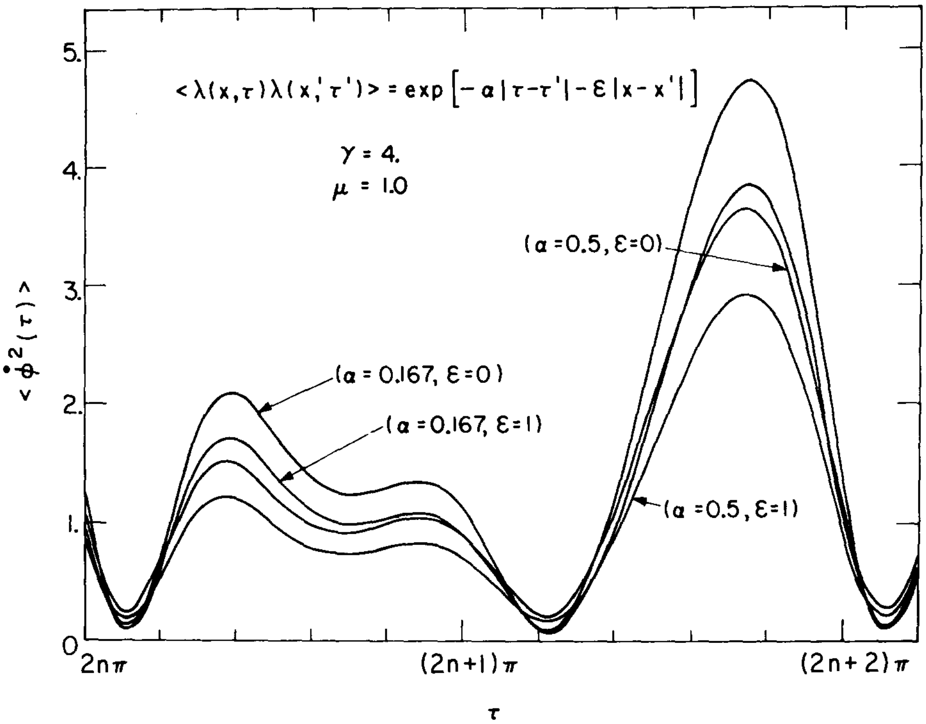

Figure 4. Meansquare flapping velocity (μ = 1.0).

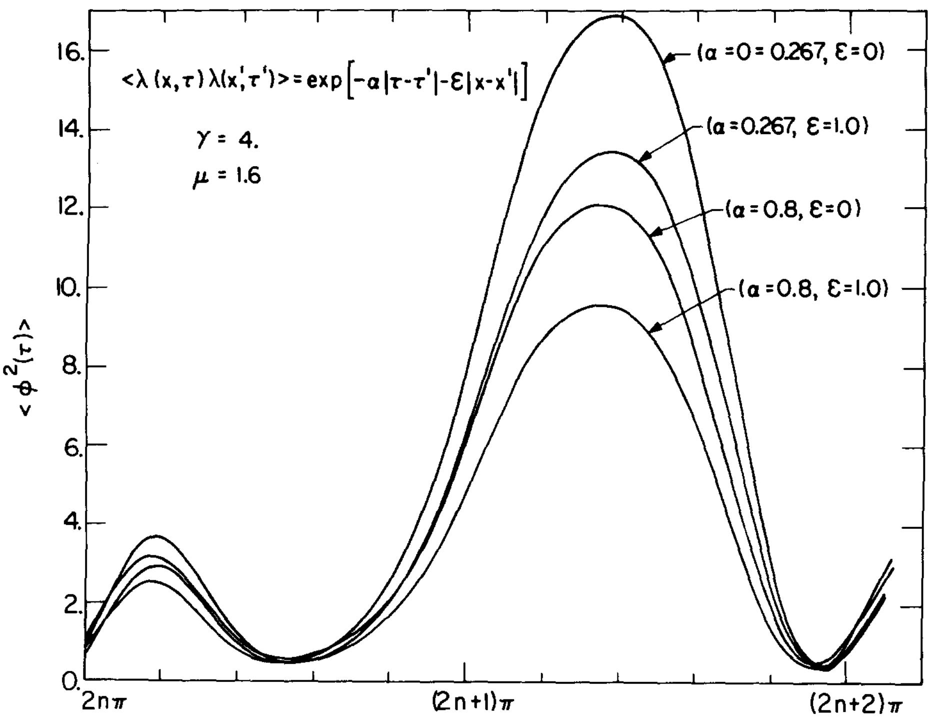

Figure 5. Meansquare flapping angle (μ = 1.6).

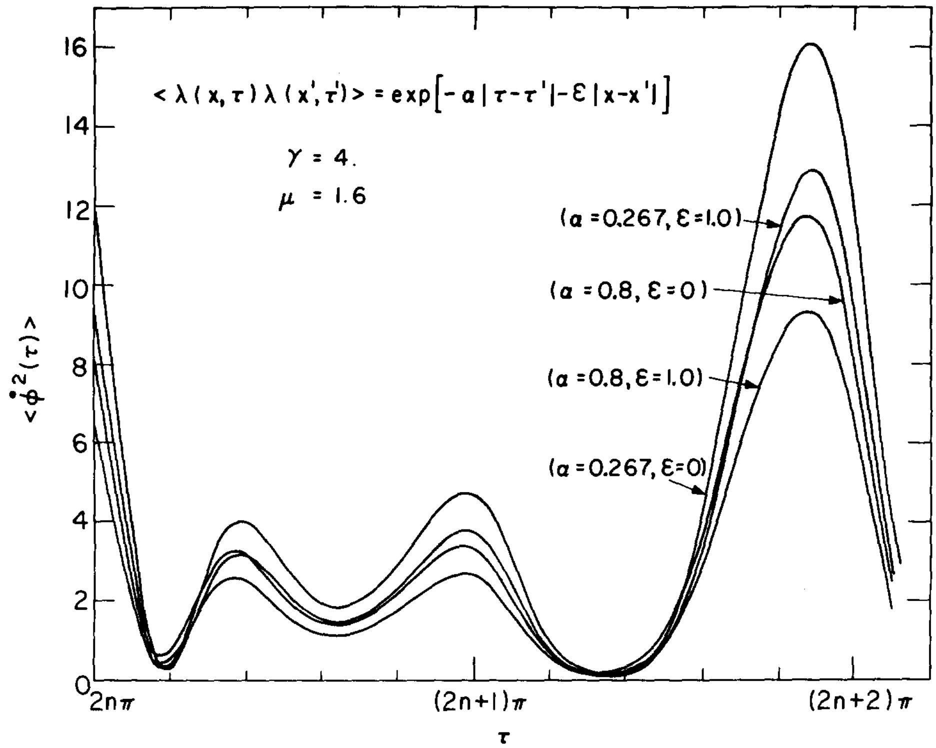

Figure 6. Meansquare flapping velocity (μ = 1.6).

TABLE 1.

Variation of Maximum $<\phi^2(\tau)>/\sigma^2$ with Lock Number for $<\lambda(x,\tau)\lambda(x',\tau')> = \sigma^2 exp(-\alpha\mid\tau-\tau'\mid - \epsilon\mid x-x'\mid)$.

		$\gamma = 2$	$\gamma = 4$	$\gamma = 8$	$\gamma = 12$
$\mu = 1.0$	$\epsilon = 1.0$	1.26	3.76	13.74	30.06
$\alpha = 0.5$	$\epsilon = 0.$	1.58	4.71	17.26	37.75
$\mu = 1.0$	$\epsilon = 1.0$	1.97	5.22	17.20	36.70
$\alpha = 0.167$	$\epsilon = 0.$	2.44	6.53	21.61	46.07
$\mu = 1.6$	$\epsilon = 1.0$	2.30	9.58	61.29	183.30
$\alpha = 0.8$	$\epsilon = 0.$	2.91	12.09	77.55	231.32
$\mu = 1.6$	$\epsilon = 1.0$	3.17	13.40	85.92	251.25
$\alpha = 0.267$	$\epsilon = 0.$	3.98	16.88	109.07	316.29

TABLE 2.

Variation of Maximum $<\dot{\phi}^2(\tau)>/\sigma^2$ with Lock Number for $<\lambda(x,\tau)\lambda(x',\tau')> = \sigma^2 exp(-\alpha\mid\tau-\tau'\mid - \epsilon\mid x-x'\mid)$.

		$\gamma = 2$	$\gamma = 4$	$\gamma = 8$	$\gamma = 12$
$\mu = 1.0$	$\epsilon = 1.0$	1.03	2.91	10.54	23.05
$\alpha = 0.5$	$\epsilon = 0.$	1.29	3.62	13.18	29.11
$\mu = 1.0$	$\epsilon = 1.0$	1.54	3.83	12.56	27.01
$\alpha = 0.167$	$\epsilon = 0.$	1.89	4.72	15.59	33.99
$\mu = 1.6$	$\epsilon = 1.0$	1.62	9.20	75.01	246.14
$\alpha = 0.8$	$\epsilon = 0.$	2.05	11.72	95.34	312.56
$\mu = 1.6$	$\epsilon = 1.0$	2.08	12.77	103.90	331.84
$\alpha = 0.267$	$\epsilon = 0.$	2.60	16.05	137.23	423.09

7. Autocorrelation functions

Having determined (the rigid flapping mode approximation for) U, S and V, we can now calculate the autocorrelation of the flapping angle $\phi(t)$ which characterizes the second-order statistics of the flapping response. We begin by multiplying (1) by $w(x',\tau')$ and ensemble-averaging the result to get

$$R_{\tau\tau} + \gamma_0 | x + \mu\sin\tau | R_\tau + L_{x\tau}[R] = \gamma_0 | x + \mu\sin\tau | \Lambda(x,\tau;x',\tau') \tag{56}$$

where

$$\begin{aligned} R(x,\tau;x',\tau') &= \langle w(x,\tau)w(x',\tau')\rangle, \\ \Lambda(x,\tau;x',\tau') &= \langle \lambda(x,\tau)w(x',\tau')\rangle. \end{aligned} \tag{57}$$

To get the yet unknown load-response correlation Λ, we multiply (5) through by $w(x',\tau')$ and ensemble average giving us

$$\Lambda_\tau + \alpha\Lambda = \sqrt{2\alpha}\langle n(x,\tau)w(x',\tau')\rangle = 0, \quad (\tau > \tau') \tag{58}$$

where the right-hand side vanishes for $\tau > \tau'$ by (6). At $\tau = \tau'$, we have from the relevant definitions

$$\Lambda(x,\tau';x',\tau') = p(x,x',\tau') \equiv \langle \lambda(x,\tau')w(x',\tau')\rangle. \tag{59}$$

It follows from (11), (25), (58), (59) and the assumption of rigid flapping that

$$\bar{\Lambda}_\tau + \alpha\bar{\Lambda} = 0 \big| (\tau > \tau'), \quad \bar{\Lambda}(x,\tau';\tau') = \bar{p}(x,\tau') \tag{60}$$

where

$$\bar{\Lambda}(x,\tau;\tau') = 3\int_0^1 x'\Lambda(x,\tau;x',\tau')dx' = \langle \lambda(x,\tau)\phi(\tau')\rangle. \tag{61}$$

She solution of (60) is

$$\bar{\Lambda}(x,\tau;\tau') = \bar{p}(x,\tau')e^{-\alpha(\tau-\tau')}, \quad (\tau \geqslant \tau'). \tag{62}$$

Upon introducing the rigid flapping assumption into (56), we get

$$\tilde{R}_{\tau\tau} + c(\tau)\tilde{R}_\tau + [\omega^2 + k(\tau)]\tilde{R} = \tilde{\Lambda}(\tau,\tau') \quad (\tau > \tau') \tag{63}$$

where $\tilde{R}(\tau;\tau') = \langle \phi(\tau)\phi(\tau')\rangle$ and

$$\begin{aligned} \tilde{\Lambda}(\tau;\tau') &= 3\gamma_0\int_0^1 x\,| x + \mu\sin\tau |\,\bar{\Lambda}(x,\tau;\tau')dx \\ &= 3\gamma_0 e^{-\alpha(\tau-\tau')}\int_0^1 x\,| x + \mu\sin\tau |\,\bar{p}(x,\tau')dx \\ &\equiv \tfrac{1}{2}\gamma e^{-\alpha(\tau-\tau')}\tilde{P}(\tau;\tau') \end{aligned} \tag{64}$$

with $\widetilde{P}(\tau';\tau') = P(\tau')$ according to (24). Note that

$$\widetilde{R}(\tau';\tau') = \langle \phi^2(\tau') \rangle = U(\tau'), \quad \widetilde{R}_\tau(\tau';\tau') = S(\tau'), \tag{65}$$

$$\widetilde{R}_{\tau\tau'}(\tau';\tau') = V(\tau'). \tag{66}$$

The two conditions in (65) serve as initial conditions for (63). But even without solving the initial-value problem (63) and (65) explicitly for $\widetilde{R}(\tau;\tau')$, the following informative observation can be made. Since the effect of a spatial load correlation appears only in $\widetilde{P}(\tau;\tau')$ which is a periodic function of τ and τ' at steady state, the correlation time of the response depends only on the parameters α and γ and not on ϵ. Within the framework of rigid flapping, our particular type of spanwise load correlation only modifies the amplitude of the autocorrelation of the response.

8. Multi-mode solutions

The key step in the spatial correlation method [3] used in this paper for the second-order response statistics of stochastic rotor blade response is the determination of the four spatial correlation functions $u(x,y,\tau)$, $s(x,y,\tau)$, $t(x,y,\tau)$ and $v(x,y,\tau)$ defined in (7). For a class of random excitations including the type considered in this paper, this is done by the procedure outlined in Section 2. In later sections, we used this procedure and obtained an approximate solution for these spatial correlation functions by limiting ourselves to a rigid flapping mode of blade deformation. This approximate solution shows that the second-order statistics of the rigid flapping mode response may vary considerably with the finite correlation length of the spatially nonuniform random excitation.

More accurate second-order blade response statistics can be obtained by allowing for the contribution of other rotating beam modes. Let $W_k(x)$, $k = 0, 1, 2, \ldots$, be the orthonormal eigenfunctions of the operator $L_x[\ ] \equiv \zeta^4[\ ]_{xxxx} - \frac{1}{2}(1 - x^2)[\ ]_{xx} + x[\ ]_x$ with the hinged-free end conditions (3) and $\{\omega_k^2\}$ be the corresponding eigenvalues (with $W_0(x) = \sqrt{3}\,x$ and $\omega_0^2 = \omega^2 = 1$). Analytical and numerical solutions for this eigenvalue problem can be found in [6], [10]* and elsewhere. With

$$\{p(x,y,\tau), q(x,y,\tau), u(x,y,\tau), \ldots, v(x,y,\tau)\}$$
$$= \sum_{m=0}^{K} \sum_{n=0}^{K} \{p_{mn}(\tau), q_{mn}(\tau), U_{mn}(\tau), \ldots, V_{mn}(\tau)\} W_m(x) W_n(y) \tag{67}$$

for some fixed K, we get from (17)-(19) K uncoupled initial value problems for $\{p_{mn}(\tau)\}$ and $\{q_{mn}(\tau)\}$ each involving $2K$ ODE,

$$\dot{p}_{mn} + \alpha p_{mn} = q_{mn}, \tag{68}$$

* The solutions obtained in [10] and related articles are for a clamped-free rotating beam. However, the method employed there can also be used for a hinged-free beam.

$$\dot{q}_{mn} + \alpha q_{mn} = \omega_n^2 p_{mn} - \sum_{j=0}^{K} (\eta_{nj} p_{mj} + \xi_{nj} q_{mj}) + R_{mn}(\tau); \tag{69}$$

$$p_{mn}(0) = q_{mn}(0) = 0, \tag{70}$$

$(m, n = 0, 1, 2, \ldots, K)$ where

$$\xi_{nj}(\tau) = \gamma_0 \int_0^1 | y + \mu \sin\tau | W_n(y) W_j(y) dy = \xi_{jn}(\tau), \tag{71}$$

$$\eta_{nj}(\tau) = \gamma_0 \mu \cos\tau \int_0^1 | y + \mu \sin\tau | W_n(y) W_j'(y) dy \quad (\neq \eta_{jn}). \tag{72}$$

$$R_{mn}(\tau) = \gamma_0 \int_0^1 \int_0^1 | y + \mu \sin\tau | R_s(x,y) W_m(x) W_n(y) dy dx = R_{nm}(\tau). \tag{73}$$

Note that the expressions for p and q in (67) automatically satisfy the boundary conditions (20). We also get from (8), (10), (12), (13) and (15) the following initial value problem for $4K^2$ coupled ODE for the determination of $\{U_{mn}\}$, $\{T_{mn}\}$, $\{S_{mn}\}$ and $\{V_{mn}\}$:

$$\dot{U}_{mn} = T_{mn} + S_{mn}, \tag{74}$$

$$\dot{T}_{mn} = V_{mn} + \omega_m^2 U_{mn} - \sum_{k=0}^{K} (\eta_{mk} U_{kn} + \xi_{mk} T_{kn}) + P_{mn}(\tau), \tag{75}$$

$$\dot{S}_{mn} = V_{mn} + \omega_n^2 U_{mn} - \sum_{k=0}^{K} (\eta_{nk} U_{mk} + \xi_{nk} S_{mk}) + P_{nm}(\tau), \tag{76}$$

$$\dot{V}_{mn} = \omega_m^2 S_{mn} + \omega_n^2 T_{mn} - \sum_{k=0}^{K} (\eta_{mk} S_{kn} + \eta_{nk} T_{mk} + \xi_{mk} V_{kn} + \xi_{nk} V_{mk}) + Q_{mn}(\tau); \tag{77}$$

$$U_{mn}(0) = S_{mn}(0) = T_{mn}(0) = V_{mn}(0) = 0, \tag{78}$$

$(m, n = 0, 1, \ldots, K)$ where

$$P_{mn}(\tau) = \gamma_0 \sum_{j=0}^{K} p_{jn}(\tau) \int_0^1 | x + \mu \sin\tau | W_j(x) W_m(x) dx \quad (\neq P_{nm}(\tau)), \tag{79}$$

$$Q_{mn}(\tau) = \gamma_0 \sum_{j=0}^{K} \left\{ q_{jn}(\tau) \int_0^1 | x + \mu \sin\tau | W_j(x) W_m(x) dx + q_{jm}(\tau) \int_0^1 | x + \mu \sin\tau | W_j(x) W_n(x) dx \right\} = Q_{nm}(\tau). \tag{80}$$

Note that the expressions for the spatial correlations functions in (67) automatically satisfy the boundary conditions (16).

It remains to use eigenfunction expansions to determine the autocorrelation function of the blade displacement. With (67) the solution of (58) and (59) takes the form

$$\Lambda(x,\tau;x',\tau') = p(x,x',\tau')e^{-\alpha(\tau-\tau')}$$
$$= e^{-\alpha(\tau-\tau')} \sum_{m=0}^{K} \sum_{n=0}^{K} p_{mn}(\tau')W_m(x)W_n(x') \tag{81}$$

for $\tau \geqslant \tau'$. Correspondingly, we set

$$R(x,\tau;x',\tau') = \sum_{m=0}^{K} \sum_{n=0}^{K} r_{mn}(\tau,\tau')W_m(x)W_n(x') \quad (\tau \geqslant \tau') \tag{82}$$

and we get from (56) and the initial conditions $R(x,\tau';x',\tau') = U(x,x',\tau')$ and $R_\tau(x,\tau';x',\tau') = T(x,x',\tau')$ the following initial value problem for $r_{ij}(\tau,\tau')$, $i, j = 0, 1, 2, \ldots, K$:

$$r_{ij,\tau\tau} - \lambda_i^2 r_{ij} + \sum_{m=0}^{K} (\eta_{im} r_{mj} + \xi_{im} r_{mj,\tau})$$

$$= e^{-\alpha(\tau-\tau')} \sum_{m=0}^{K} \xi_{im} p_{mj} \quad (\tau > \tau'), \tag{83}$$

$$r_{ij}(\tau',\tau') = U_{ij}(\tau'), \quad r_{ij,\tau}(\tau',\tau') = T_{ij}(\tau'). \tag{84}$$

Evidently an approximate solution for the second-order response statistics with a specified degree of accuracy can be obtained by taking K sufficiently large in the above normal mode-Galerkin procedure. The rigid flapping solution corresponds to the $K = 0$ case and was found to be a reasonably accurate approximation of the exact solution for a spatially uniform random excitation [7, 8]. Whether it is a good approximate solution for blades with a (zero mean) spatially nonuniform random excitation depends on the load correlation length to blade length ratio. Note that the amount of machine computation increases geometrically with K and that a direct numerical solution of the initial boundary value problems of Section 2 (as done in [2] for blades with no bending stiffness) may be more economical for large values of K. If an accurate solution can be obtained with a small number of eigenfunctions, the present normal mode approach has the advantage of singling out the dominant rotating beam modes in the blade response. In the case of $K = 0$, it also has enabled us to understand the qualitative dependence of the blade response on the load correlation length, at least in the case of a small advance ratio.

Acknowledgement

The author is grateful to the Applied Mathematics Group and the Department of Aeronautics and Astronautics of the University of Washington for the use of their research facilities. He is also grateful to his friend C. Lakshmikantham who introduced him to stochastic problems in rotor blades and provided him with the initial support to work on them.

REFERENCES

[1] P. Friedmann and P. Tong, Dynamic nonlinear elastic stability of helicopter rotor blades in hover and forward flight, *NASA* CR-114485, May 1972.

[2] F. Y. M. Wan and C. Lakshmikantham, The spatial correlation method and a time-varying flexible structure, presented at AIAA-ASME Structural Dynamics and Materials Conference, Williamsburg, Va., 1973; *AIAA J.* 12 (1974) 700-704.

[3] F. Y. M. Wan, A direct method for linear dynamical problems in continuum mechanics with random loading, presented at the 13th Intern'l Congr. of Theor. & Appl. Mech., Moscow, USSR, 1973; also *Studies in Appl. Math.* 52 (1973) 259-275.

[4] G. H. Gaonkar and K. H. Hohenemser, Stochastic properties of turbulence excited rotor blade vibrations, *AIAA J.* 9 (1971) 419-424.

[5] F. Y. M. Wan and C. Lakshmikantham, Rotor blade response to random loads: a direct time domain approach, *AIAA J.* 11 (1973) 24-28.

[6] F. Y. M. Wan, An in-core finite difference method for separable boundary value problems on a rectangle, *Studies in Appl. Math.* 52 (1973) 103-113.

[7] C. Lakshmikantham and F. Y. M. Wan, An algebraic method for linear dynamical systems with stationary excitations, *J. Sound and Vibration* 20 (1973) 105-120.

[8] G. H. Gaonkar and K. H. Hohenemser, Flapping response of lifting rotor blades to atmospheric turbulence, *J. of Aircraft* 6 (1969) 496-503.

[9] G. J. Sissingh, Dynamics of rotors operating at high advance ratios, *J. of Helicopter Society* 13 (1968) 56-63.

[10] W. D. Lakin, On the differential equation of a rapidly rotating slender rod, *Quart. Appl. Math.* 32 (1974) 11-27.